Journal Home Page: https://sjes.univsul.edu.iq/

Research Article:

Characterization and Volumetric Stability of High-Plasticity Clay Stabilized by Fly Ash and Metakaolin Based Geopolymers

Chra Othman Mahmood [1,a]
Zahraa Noori Rashied [2,a,*]

[a] **Department of Geotechnical Engineering, Faculty of Engineering, Koya University, Koya, KR,Iraq**

Article Information

Article History:
Received: March 3rd , 2026
Accepted: April 30th,2026
Available online: April ,2026

Keywords:
CH clay soil, Geopolymer, Fly ash, Metakaolin, Alkali activator, Soil improvement, Microstructure.

Corresponding author:
Zahraa Noori Rashied
E-mail: zahraa.noori@koyauniversity.org
Researcher Involved:
Chra Othman Mahmood
E-mail: chra.othman@koyauniversity.org

DOI https://doi.org/10.17656/sjes.10213

Abstract

This study aims to characterize and analyze the physical and chemical performance of CH clay soil stabilized independently and separately by fly ash and metakaolin based geopolymers activated by sodium hydroxide. Different percentages up to 18% of both geopolymers were considered to assess how they affect soil plasticity, compaction and volumetric stability. The X-ray fluorescence (XRF) analysis for soil and binders were conducted to assess aluminosilicate amounts necessary for geopolymer formation and to support the observed results. The results of Atterberg's limits and compaction tests showed a decrease in soil plasticity and increase in maximum dry density of soil with increase in geopolymer content. Durability was evaluated through one-dimensional swelling-shrinkage cycles, where higher binder contents resulted in pronounced volume change reduction and hence improvement of dimensional stability due to moisture changes. Scanning electron microscopy analysis showed a dense and compact matrix with continuous geopolymer gel formation and enhanced interparticle bonding. The findings of these tests show that sodium hydroxide activated geopolymer binders can alter the physio-chemical properties and matrix of clay soil to improve its dimensional stability and wetting-drying cycle durability.

1. Introduction

Geopolymer technology has been developed as a sustainable and eco-friendly substitute for traditional soil stabilizers like cement and lime. Clay soils, and more specifically high plasticity clays (CH), have been well-documented to possess poor engineering behavior, characterized by high shrink-swell ratios, low bearing capacity, and instability in terms of volumes due to changes in the soil's moisture content [1, 2]. High-plasticity clays containing montmorillonite undergo changes in volumes due to the sensitivity of the soil to changes in the soil's moisture content, increasing in volumes when exposed to water and shrinking when dried. This phenomenon results in irregular deformation of the soil, thus posing a serious risks to the sustainability and functionality of the underlying foundations and pavements [3]. Lime and cement have been the most widely accepted traditional methods in the improvement of the behavior of expansive soils [4]. A substantial amount of research work has confirmed the effectiveness of lime and cement in improving the adverse properties of expansive soils by decreasing the plasticity index, free swell, and shrink-swell properties of the soil [5-7]. Conventional soil stabilizers like cement and lime work well for upgrading soil properties, are associated with high energy consumption and significant greenhouse gas emissions. The cement industry alone is believed to

be responsible for around 7–8% of overall anthropogenic CO_2 emissions, primarily for limestone calcination and energy-intensive clinker production [8-12]. Using ordinary Portland cement to stabilize soil causes significant environmental problems, and these problems are now considered serious. Therefore, a more environmentally friendly and effective method for soil stabilization has emerged with the use of geopolymer binder materials that minimize CO_2 emissions without sacrificing stabilization performance [13]. Geopolymers are alkali-activated aluminosilicate materials formed through the dissolution and polycondensation of silica (SiO_2) and alumina (Al_2O_3) species in a high-pH environment [13-15]. In this study, sodium hydroxide (NaOH) alone was used as the activating solution to promote the formation of sodium aluminosilicate hydrate (N–A–S–H) gels that enhance bonding and durability. Fly ash, a by-product of coal combustion and metakaolin, a calcined form of kaolinite, serve as aluminosilicate precursors that undergo dissolution and reprecipitation reactions to form a rigid, amorphous network [13, 16-19]. The most common calcined aluminosilicate materials used for geopolymers are metakaolin and coal fly-ash, The N–A–S–H (sodium–aluminosilicate–hydrate) gel model typically originates from the alkali activation of low-calcium, aluminosilicate-rich materials such as fly ash and metakaolin, which polymerize into a three-dimensional amorphous network exhibiting strong bonding and structural integrity [11]**.** The geopolymerization process produces a gel that binds the particles of the soils together, hence affecting the micro-structure and mineralogy of the soil, which ultimately improves its mechanical properties [20, 21]. Even though earlier studies proved the geopolymerization technique using mixtures of activators such as sodium silicate and NaOH on soils has the capability for stabilization, which makes it difficult to identify the separate effects of hydroxide ions to the kinetics of geopolymerization.

This study aims to enhance the understanding of NaOH-activated geopolymer mechanisms in soil stabilization and to support their adoption as sustainable, low-carbon alternatives to conventional binders and methods. The novelty of this work lies in isolating the effect of NaOH activation and examining its role in geopolymer gel formation, soil structure modification, and volumetric stability under wetting–drying cycles. The percentages of geopolymer binders used in this study were 6%, 10%, 14%, and 18%, which were added to the clay soils to examine their effects on its physical and chemical characteristics. The tests conducted in this study to examine clay soils include Atterberg limits, compaction and swelling-shrinkage tests to assess soil plasticity, density, and volumetric stability. The chemical composition of geopolymer was identified using X-ray fluorescence (XRF), while scanning electron microscopy (SEM) was conducted to examine geopolymer gel formation, particle bonding, and pore structure of the stabilized high plasticity clay.

2. Materials and methods

2.1 preparation of high plasticity Clay Soil

High plasticity clay soil used in this study was prepared to simulate the behavior of expansive soil. The soil sample was collected from a depth of about 1 meter below ground level. First, the soil samples were placed in thin layers and exposed to sunlight for air-dry over a period of two months. After oven drying, the soil samples were crushed manually and sieved through 4.75 mm (No. 4) IS sieve. Then, the natural soil was artificially modified by the addition of 20% bentonite clay powder (mass replacement method) as an effort to increase the clay content (see Figure1e), so the soil's plasticity and swelling potential replicate the plastic characteristics of highly expansive soils (CH type). In order to obtain a uniform color and texture, the materials were manually combines and added gradually. After preparation of the artificial soil, the physical and chemical properties were evaluated in accordance to ASTM slandered as demonstrated in Table 1. The results analysis occupied that the soil can be classified as a high-plasticity clay (CH) according to the Unified Soil Classification System (USCS).

2.2 Fly ash class (F)

The fly ash used in this study is a Class F fly ash (see Figure 1a), conforming to the standards of ASTM C618. Class F fly ash is primarily produced from the burning of anthracite coal, bituminous coal, or a combination of both, characterized by a low calcium content (<10% CaO) and a high siliceous and aluminous component. The combined content of SiO_2, Al_2O_3, and Fe_2O_3 in the fly ash used was above 70% (see table 2), that satisfying the criteria for a low calcium pozzolanic material [22]. The high amorphous aluminosilicate content provides the reactive component for the geopolymerization reaction when the fly ash is activated with an alkaline liquid solution [15, 23]. The fly ash, according to the manufacturer's data, has a fine, spherical particle shape, where less than 34% of the particles are retained in the 45 µm sieve, which indicating that the particles are mostly below 45 µm in size. A particle size of this nature is beneficial for increased reactivity, providing a larger surface area, thus facilitating the easy dissolution of the silicon and aluminum components when the fly ash is activated with the alkali solution [24].

2.3 Metakaolin

Metakaolin was used as a highly reactive pozzolanic material obtained by calcining kaolin clay at 650–800°C [15, 25]. It is fine and white as shown in Figure

1b. Based on the manufacturer's specifications (see Figure 2), the metakaolin is characterized by a high whiteness of approximately 93–94%, indicating a high degree of purity content, and ultrafine particle sizes of 2000 and 4000 mesh. This fine particle size enhances dispersion within the soil matrix and promotes efficient interaction with the alkaline activator during geopolymerization. The high fineness facilitates the dissolution of reactive silica and alumina, and contributes to the formation of a dense geopolymer gel, which binds soil particles and reduces plasticity and swelling potential. This makes it an effective additive for improving the mechanical and microstructural properties of expansive soils. Chemical composition analysis (see table 2) show that metakaoline used in this study contain major oxide components more than 70% that met low calcium pozzolanic materials [22].

2.4 Artificial soil, fly ash and metakaolin chemical compositions:

The X-ray fluorescence (XRF) analysis was conducted in this study and the chemical content of the CH soil, fly ash, and metakaolin were as given in Table 2. SiO_2, AlO_3, CaO, FeO_3 identified as major oxide components, and the rest categorized as minor constituents. The chemical composition analysis indicates that artificial high plasticity clay used in this study contain about 85 % of major oxide components (high silica and moderate alumina content), indicating an aluminosilicate-rich clay mineralogy suitable for alkali activation index [20, 26]. While both fly ash and metakaolin contain rich amounts of major oxide components exceeding 90%, confirming their strong pozzolanic potential. The low CaO content in both binder materials suggests that stabilization will primarily occur through geopolymeric N-A-S-H gel formation rather than traditional C-S-H mechanisms [27, 28]. The use of NaOH as the sole alkali activator promotes dissolution of silica and alumina from fly ash, metakaolin, and the CH soil matrix. Metakaolin is expected to exhibit higher early reactivity compared to fly ash because of its amorphous structure and finer particle size [29, 30]. Although the absence of sodium silicate may limit the availability of soluble silicate species, sufficient geopolymeric bonding can still be achieved through prolonged curing and optimized NaOH concentration [29].

2.5 Alkaline Solution

Sodium hydroxide (NaOH) is commonly used in geopolymer studies due to its high alkalinity, availability, and strong ability to promote aluminosilicate dissolution [31]. In this respect. The alkaline environment helps in breaking Si-O-Si bonds as well as Al-O-Si bonds in aluminosilicate compounds through hydroxide ions (OH^-), which are present in the solution of sodium hydroxide (NaOH), leading to the release of Si and Al species in the aqueous phase [15]. The present research work has used 10 M concentration of sodium hydroxide solution in the synthesis of geopolymer material, following the concentration that has been used in previous research work in the activation of aluminosilicate components [32-36]. The required quantity of NaOH pellets (see Figure 1d), 400 g was gradually added to tap water in a glass container and making up the final volume to 1 L. The solution was left for 24 hours to ensure complete dissolution (see Figure 1c). The solution was occasionally stirred for a consistent mixture. The concentration of NaOH was consistent for all geopolymer mixtures used in this study. The prepared solution is shown in fig 1. Due to the highly caustic nature of NaOH, all handling was performed under strict safety precautions. Personal protective equipment, including gloves, goggles, and a lab coat, was worn. Additionally, the entire process was carried out in a well-ventilated environment to avoiding splashes and inhalation of fumes. The resulting solution was stored in a tightly sealed, labeled glass container to prevent accidental contact and moisture absorption. This 10 M NaOH solution provided the necessary hydroxide ions for the activation of the fly ash and metakaolin, resulting in the geopolymer gel and improving the mechanical and microstructural properties of treated soils [37, 39].

3. Methods of testing

3.1 Atterberg Limits Test

Characteristics of the plasticity of the geopolymer-stabilized (CH) soil were determined by the Atterberg tests. The tests were conducted 2 hours after the addition of the geopolymer with the soil, allowing for the homogenous mixing and preventing the premature hardening and evaporation of the moisture that could influence the results. 250 g of the CH soil was used for each test sample consisting of 20% bentonite clay powder and 80% natural soil passing sieve No. 40. Then the required proportions of fly ash or metakaolin were then added to the soil, mixed thoroughly, and uniformly distributed throughout the mixture. Subsequently, 165 g of 10 M sodium hydroxide (NaOH) solution was added to each mixture to achieve a consistency below the liquid limit, suitable for Atterberg limit testing. The liquid limit test utilized the electrical Casagrande cup method (see Figure 3a) is to achieve 25 drops as specified in the ASTM D4318 standard. During preparation, an equal quantity of 10 M sodium hydroxide solution was added to each geopolymer–soil mixture to maintain consistency among samples. Incremental addition of the alkaline activator was strictly avoided, as any variation in the amount of alkali activator between samples could alter the degree of geopolymerization and produce inaccurate or misleading LL values. The plastic limit (PL) was measured by rolling soil threads to a 3.2 mm diameter (see Figure 3b), then the

plasticity index (PI) was calculated. The resulting Atterberg limits were used to classify the soil according to the Unified Soil Classification System (USCS) and to evaluate the influence of geopolymer stabilization on soil plasticity.

3.2 Compaction test:

The compaction characteristics of the untreated soil, fly ash and metakaolin- geopolymer-treated soils were determined using the standard proctor compaction test in accordance with ASTM D698 to obtain the maximum dry density (MDD) and optimum moisture content (OMC) for all mixtures. In this study, the preparation process began by mixing 80% natural soil with 20% bentonite manually until a uniform blend was achieved. Afterward, the required proportion of fly ash was added to the soil–bentonite mixture and mixed thoroughly by hand to ensure homogeneity. Then, the prepared alkaline activator solution (10 M sodium hydroxide) was spread over the dry mixture, mixed manually until a uniform mass was obtained, immediately after mixing, compaction was performed using an electrical compaction machine in accordance with the Standard Proctor procedure. Immediate compaction was essential because any delay in compaction leads to a reduction in maximum dry density, as the early geopolymerization reaction begins and causes partial stiffening of the mix before placement[40]. Each specimen was compacted in three equal layers, each receiving 25 blows. This procedure was repeated for all fly ash and metakaolin percentages to evaluate the influence of geopolymer content on soil compaction behavior.

3.3 Swell-Shrink Cycles Test

Swell-shrink potential tests were carried out using a one-dimensional (1-D) consolidation free swell test in accordance with ASTM D4546. In this study one dimensional consolidation ring of 6 cm in diameter and 2 cm in height was pressed through compacted soil prepared at maximum dry density and optimum moisture content for all untreated and fly ash or metakaolin-geopolymer treated soil up to 18%. After that, the ring was carefully extracted from the compacted soil sample to maintain uniformity and avoid structural disturbance. Immediately after extraction, each specimen with rings was tightly wrapped with multiple layers of falcon film to prevent moisture loss. All wrapped specimens with rings were then cured for 28 days at room temperature to allow full hydration and geopolymerization. A thermocol box was used as the curing chamber to avoid moisture loss during the curing process. After 28 days of curing, the specimens were unwrapped and the falcon film was removed, then specimens were placed in a consolidation cell between two porous stone with a loading plate on the upper porous stone. The dial gauge attached to the consolidation cell for measuring vertical deformation (ΔH) during various wet-dry cycles under a seating pressure of 1 kPa, as shown in Figure 4 (a, b and c). Specimens were subjected to six wetting and drying cycles, in wetting cycle, the samples were filled with a tap water and allowed the samples for fully swelling till no more volume increase achieved as no further vertical deformation recorded. When swelling was completed (after one week duration). After the wetting cycle, water was carefully removed from the sides of the consolidation cell using a needle and syringe, while the sample remained in the cell and its structure was not disturbed. Shrinkage was then measured in situ by monitoring the sample height with a dial gauge, and the sample was dried in a controlled environment at 40 °C ± 5 °C in a closed area. Shrinkage was considered complete when the dial gauge readings stopped decreasing or no measurable deformation was recorded. This temperature simulates field-like environmental conditions.

3.4 Scanning Electron Microscopy (SEM)

Scanning Electron Microscopy (SEM) was conducted to investigate the microstructural characteristics of the natural high plasticity soil and the geopolymer-stabilized specimens containing 18% fly ash–based geopolymer **and** 18% metakaolin-based geopolymer. All specimens selected for SEM analysis were prepared and compacted at maximum dry density (MDD)**.** The analysis aimed to evaluate the formation of geopolymer reaction products, the bonding between soil particles, and the effects of cyclic wetting and drying on the stabilized specimens. The Scanning Electron Microscopy (SEM) analysis was conducted on samples cured for 28 days before the one-dimensional swell–shrinkage cyclic test, and after completion of six wetting-drying cycles obtained from the one-dimensional swell–shrinkage consolidation test.

4. Results and discussion:

4.1 Effect geopolymer on Liquid limit and plasticity index

The Atterberg limits, as shown in Figure 5, reveal a considerable reduction in the plasticity of CH soil with the addition of Class F Fly Ash–based geopolymer. The Liquid Limit (LL) decreased from 76.5 % for natural CH soil to 45.9% at 18% Fly Ash–based geopolymer, while the Plasticity Index (PI) reduced from 46.5% to 14.4%. Similarly, Metakaolin-based geopolymer treatment reduced LL from76.5% to 46.7 at 18% metakaolin-based geopolymer and (PI) dropped from 46.5% to 15.7%. The reaction between soil minerals and the geopolymer binder led to the formation of gel, this gel filled pore spaces and coated

clay particles, thereby limiting direct contact between water and the clay surfaces. The reduction in available surface area for water adsorption and retain water led to a noticeable decrease in the liquid limit (LL) and plasticity index (PI), indicating a reduction in the soil's plastic behavior and moisture susceptibility. Similar trends have been reported in previous studies [19, 41], confirming that increasing geopolymer content effectively reduces the Atterberg limits of expansive soils by altering their clay mineral structure and surface charge characteristics . In the plasticity chart (see Figure 6), the stabilized soil samples progressively shifted from the high plasticity **(**CH) classification zone toward the low plasticity silt **(**ML) zone with increasing fly ash and metakaolin content. This shift reflects a transition from clay dominated behavior to a more silt like response with reduced plasticity. The combined effect of chemical bonding, pores filling and reduction in clay activity explain the observed decrease in Atterberg's limits and confirm the effectiveness of geopolymer stabilization in improving the consistency characteristics of expansive CH soil.

4.2 Effect of Geopolymer on Compaction Characteristics

The compaction characteristics of CH soil showed a clear improvement after stabilization with both Fly Ash and Metakaolin based geopolymers. The maximum dry density of the treated soil was higher than of the untreated CH soil, indicating enhanced packing efficiency and reduced pore spaces. For both binders, the maximum dry density increased and optimum moisture decreased progressively with the increase in geopolymer content (see Figures 7 and 8). The improvement in density can be ascribed to the cementitious gel formed during the geopolymerization process, which fills void spaces between soil particles to form a dense matrix. Metakaolin based geopolymer exhibited slightly higher maximum dry density values compared to fly ash based geopolymer at similar replacement levels, due to its higher reactivity and finer particle size, which facilitate better coating of soil grains.

4.3 Effect of Geopolymer on swell-shrink Characteristics

The one-dimensional swell–shrink test results obtained over six wetting–drying cycles (see Figures 9, 10 and 11)**.** The results expressed in terms of height change (($\Delta h/h_o$) %) where Δh represents the change in specimen height during swelling or shrinkage and h_o is the initial specimen height**)**, clearly demonstrate the effectiveness of geopolymer stabilization in controlling volumetric instability of CH soil. The magnitude of deformation decreased progressively with increasing geopolymer content for both metakaolin- and fly ash–based systems. The CH **soil** exhibited large swell and shrinkage values throughout the test, in the first cycle, the soil showed a swell of 14.7% and shrinkage of 10.8%**,** resulting in a total $\Delta h/h_o$ of 25.5% (see Figure 9). This excessive deformation was accompanied by the formation of extensive surface cracks, as observed in the test specimen shown in Figure 12a, due to the presence of highly expansive clay minerals, during wetting, expansive clay minerals absorbed water and expanded significantly, while drying caused contraction and rearrangement of the soil fabric. Although repeated cycling led to some reduction in volume change magnitude, after six cycles, reaching total cyclic height change $\Delta h/h_o$ of approximately 16.3%**.** For the 6% geopolymer treated soil, the volume change was reduced compared to the natural soil for both fly ash and metakaolin systems; however, $\Delta h/h_o$ continued to increase with successive cycles. The total $\Delta h/h_o$ values remained relatively high, reaching approximately 5.8 – 8.6% for both fly ash and metakaolin based geopolymers as shown in Figures 10 and 11. This suggests that the geopolymer content was insufficient to form a continuous binding network capable of restraining clay particle movement. The soil fabric remained partially open allowing moisture to penetrate and induce repeated expansion and contraction. The appearance of visible cracks in the 6% geopolymer ring consolidation specimens after six cycles, as shown in the Figures (12b and 12c), that confirms that this binder content was insufficient to restrain cyclic volume change and associated tensile stresses. When the geopolymer content is 10%, it is noted that the total cyclic height change ratio $\Delta h/h_o$ showed significant reduction in values to achieve 1.73% and 3.85% in fly ash geopolymer and metakaolin geopolymer, respectively. This showed significant improvement in the soil stabilization using fly ash geopolymer and metakaolin geopolymer. Less deformation in the soil is due to the bonding between the particles and the restriction in moisture movement, leading to a more controlled swell–shrink response. Although some deformation was still experienced at the increased content. Another reduction in volumetric deformation was also observed at the 14% geopolymer mixes, total $\Delta h/h_o$ values decreasing to about 0.82-2.75% for both fly ash and metakaolin based geopolymers. It was also observed that at the maximum geopolymer dosage, which was 18%, the least volumetric change was observed, with total $\Delta h/h_o$ values of 0.4% for fly ash and 2.1% for metakaolin, demonstrating excellent resistance to cyclic volume change. This trend indicates that the soil and geopolymer system was in a stabilized volumetric condition. The dense geopolymer matrix effectively restricted the clay's volumetric expansion, reduced the pore volume and clay activities, and restricted moisture movement, which in turn suppressed the cyclic swell-shrink deformations. In

Figures (12d and 12e) there were no visible cracks in the geopolymer treated soils after completion of six cycles, which indicates better structural stability. It is clear from the above results that increasing geopolymer content effectively reduces cyclic volume change and crack formation in expansive soils, and a low geopolymer content of 6% is not effective in preventing crack formation and considerable deformations. However, geopolymer content of 14% and 18% is effective in providing effective long-term swell-shrink behavior modification. Fly ash based geopolymer consistently provided lower $\Delta h/h_0$ values than metakaolin based geopolymer.

4.4 Microstructural analysis

Scanning Electron Microscopy (SEM) was employed to compare the microstructural characteristics of untreated CH soil**,** CH soil stabilized with 18% fly ash based geopolymer, and CH soil stabilized with 18% metakaolin based geopolymer**,** both before and after six swell-shrink cycles. The investigation was designed to clarify how geopolymerization modifies the soil fabric, how the aluminosilicate gel phases evolve, and how these microstructural changes correlate with the material's durability under cyclic environmental stress. The SEM images of the untreated CH soil prior to wetting–drying cycles, prepared at maximum dry density, reveal a dense and compact microstructure characterized by closely packed, plate-like clay particles arranged in a layered configuration as shown in Figure 13a. The compaction process effectively reduced visible macropores and forced the clay platelets into closer contact, resulting in a relatively uniform and continuous fabric with limited pore spaces. This compact, layered microstructure is primarily the result of mechanical densification at maximum dry density**,** rather than any form of chemical cementation. Despite this apparent compactness, the interparticle bonding within the CH soil remains inherently weak, as it is governed predominantly by physicochemical forces such as electrostatic attraction and van der Waals interactions rather than durable cementitious bonds. The apparent continuity of the matrix therefore does not imply long-term resistance to environmental actions. In fact, the oriented clay fabric formed during compaction can enhance anisotropy and facilitate moisture movement along particle planes once wetting occurs. The presence of expandable clay minerals such as montmorillonite and smectite allows for the entry of water molecules to spaces that are not readily discernible at the SEM level. After the entry of water molecules, the clay particles experience interlayer swelling. This creates stresses that affect the binding force of the particles, progressively weaken particle contacts. Thus, the soil becomes vulnerable to disintegration through the swell-shrink action. After exposure to six swell-shrink cycles, significant changes in the microstructure of the CH soil were observed as shown in Figure (13b and c). The SEM images show a pronounced increase in microcracking, particle separation, and disruption of the original fabric. Repeated wetting caused swelling of the clay minerals, while subsequent drying led to shrinkage and tensile stress development. These cyclic volumetric changes resulted in the widening of pores, breakdown of particle contacts, and formation of interconnected crack networks within the soil matrix. The 18% fly ash–based geopolymer before 6 swell-shrink Cycles exhibits a dense, cohesive, and well-integrated microstructure in which soil particles are encapsulated by a continuous geopolymer gel (see Figure 13d). This effect is due to the encapsulation of the soil particles within the geopolymer gel. Additionally, there is filling and interconnection of the pore spaces within the aluminosilicate particles. This is similar to the action of cement. As a result, there is a reduction of pore-connecting spaces, this has a significant effect on reducing the pore volume available for moisture expansion, thereby limiting swelling during wetting, and this is evident from a notable reduction in the change in height ($\Delta h/h_0$). When drying occurs, the geopolymer gel matrix maintains connectivity between the particles. This is responsible for reducing shrinkage and cracks. SEM image of 18% metakaolin-based geopolymer shown in Figure (13f) also indicate a dense and cohesive matrix. This is due to the geopolymer gel, there is a notable reduction in pore connectivity. Geopolymer gel effectively binding the soil particles. This is a result of the high reactivity of metakaolin. This is responsible for a rapid geopolymerization reaction. SEM results of CH soil treated with 18% fly ash-based geopolymer and 18% metakaolin-based geopolymer subjected to six cycles of swell-shrink were obtained. As shown in Figure (13e and 13g), a dense structure was maintained by both treated soils. In both cases, the soil particles remain well-bound and encapsulated within the geopolymer gel. No evidence of compromise in the microstructure is apparent within the selected level of magnification. Pore spaces remain limited and discontinuous, suggesting that the geopolymer matrix effectively resists moisture-induced degradation. The overall soil fabric appears stable and well-integrated, with no clear evidence of severe cracking or structural breakdown following swell-shrink cycles. The persistence of a compact geopolymer matrix after cyclic exposure supports the improved durability and reduced swell–shrink behavior observed in the corresponding microscopic test results.

5. Conclusions

The geopolymer stabilization method using fly ash and metakaolin assessed in terms of its effectiveness in improving the behavior of expansive soil (CH)

through consistency limits, compaction characteristics, one-dimensional swell-shrink through six cycles, and SEM tests carried out prior to and following exposure to cyclic tests. The conclusions drawn in this study are as follows:

1. The addition of geopolymer binder resulted in a significant decrease in the liquid limit (LL) as well as the plasticity index (PI) for the CH soil (LL decreased from 76.5% to 45.9% and PI from 46.5% to 14.4% for Fly Ash–based geopolymer, and LL from 76.5% to 46.7% and PI from 46.5% to 15.7% for Metakaolin–based geopolymer), indicating a decrease in clay activity as well as moisture content. After geopolymer binder addition to the soils, the soils showed movement towards the ML/OL zones from the CH zone on the plasticity chart, confirming that geopolymer stabilization effectively transforms highly plastic clay into a more stable, silt-like material.
2. The geopolymer stabilization has modified the compaction behavior of CH soils. Increasing the amount of binder used led to an increase in the dry density (MDD increased from 15.06 kN/m³ for untreated soil to up to 16.17 kN/m³ for Fly Ash–based geopolymer and 16.38 kN/m³ for Metakaolin–based geopolymer) and a reduction in the optimum moisture content (OMC decreased from 24.7% to ~20.1% for Fly Ash–based geopolymer and to ~20.55% for Metakaolin–based geopolymer) of the CH soils
3. Soils with untreated CH showed a marked swell–shrink deformation under cyclic loading, with total $\Delta h/h_0$ of 25.5% in the first cycle and approximately 16.3% after six cycles. Conversely, soils with added geopolymers showed a marked reduction in volumetric deformation $\Delta h/h_0$, with 6% binder content reducing $\Delta h/h_0$ to 5.8–8.6%, 10% to 1.73–3.85%, 14% to 0.82–2.75% for both fly ash– and metakaolin-based geopolymers, and 18% achieving the lowest $\Delta h/h_0$ of 0.4% for fly ash and 2.1% for metakaolin. Higher binder contents showed higher soil stabilities, and geopolymers made from fly ash exhibited higher resistance against cyclic moisture-induced deformation compared to metakaolin-based geopolymers.
4. SEM analysis revealed that the untreated CH soil, although dense at maximum dry density before cycling, suffered significant microstructural degradation after swell-shrink cycles, including cracking, particle separation, and increased pore connectivity. In contrast, geopolymer-stabilized soils developed dense and cohesive microstructures prior to cycling due to the formation of gel. After six swell-shrink cycles, both geopolymer systems maintained improved structural integrity, characterized by a dense and cohesive microstructure with limited pore development, resulting in enhanced volumetric stability compared to untreated CH soil.
5. Future studies should evaluate the mechanical strength parameters (e.g., unconfined compressive strength, shear strength) of geopolymer-stabilized soils under long-term cyclic moisture conditions and explore the combined effects of varying soil types, geopolymer ratios, and curing regimes to optimize stabilization strategies for field applications.

References

[1] Nelson, J. D., & Miller, D. J. (1997). *Expansive soils: Problems and practice in foundation and pavement engineering*. John Wiley & Sons.

[2] Chen, F. H. (2012). *Foundations on expansive soils*. Elsevier.

[3] Johnson, L. D. (1969). *Review of literature on expansive clay soils*.

[4] Horpibulsuk, S., Phetchuay, C., Chinkulkijniwat, A., & Cholaphatsorn, A. (2013). Strength development in silty clay stabilized with calcium carbide residue and fly ash. *Soils and Foundations, 53*(4), 477–486.

[5] Abass, I. K. (2013). Lime stabilization of expansive soil. *Journal of Engineering and Sustainable Development, 17*, 219–232.

[6] Zumrawi, M. M., & Hamza, O. S. (2014). Improving the characteristics of expansive subgrade soils using lime and fly ash. *International Journal of Science and Research, 3*, 1124–1129.

[7] Al-Rawas, A. A., Hago, A., & Al-Sarmi, H. (2005). Effect of lime, cement and Sarooj (artificial pozzolan) on the swelling potential of an expansive soil from Oman. *Building and Environment, 40*(5), 681–687.

[8] Ige, O. E., & Kabeya, M. (2025). Decarbonizing the cement industry: Technological, economic, and policy barriers to CO_2 mitigation adoption. *Clean Technologies, 7*, 85.

[9] Andrew, R. M. (2018). Global CO_2 emissions from cement production. *Earth System Science Data, 10*, 195–217.

[10] Habert, G., De Lacaillerie, J. D. E., & Roussel, N. (2011). An environmental evaluation of geopolymer-based concrete production: Reviewing current research trends. *Journal of Cleaner Production, 19*(11), 1229–1238.

[11] Garcia-Lodeiro, I., Palomo, A., & Fernández-Jiménez, A. (2014). An overview of the chemistry of alkali-activated cement-based binders. In *Handbook of alkali-activated cements, mortars and concretes* (pp. 19–47). Woodhead Publishing.

[12] Yang, K.-H., Jung, Y.-B., Cho, M.-S., & Tae, S.-H. (2015). Effect of supplementary cementitious materials on reduction of CO_2

emissions from concrete. *Journal of Cleaner Production, 103*, 774–783.

[13] Provis, J. L., & Van Deventer, J. S. J. (2009). *Geopolymers: Structures, processing, properties and industrial applications*. Woodhead Publishing.

[14] Davidovits, J. (1991). Geopolymers: Inorganic polymeric new materials. *Journal of Thermal Analysis, 37*, 1633–1656.

[15] Mohan Kumar, S., Kinuthia, J., Oti, J., & Adeleke, B. (2025). Geopolymer chemistry and composition: A comprehensive review of synthesis, reaction mechanisms, and material properties oriented with sustainable construction. *Balance, 11*, 26.

[16] Adhikari, B., Khattak, M. J., & Adhikari, S. (2021). Mechanical and durability characteristics of fly ash-based soil–geopolymer mixtures for pavement base and subbase layers. *International Journal of Pavement Engineering, 22*(9), 1193–1212.

[17] Khadka, S. D., Jayawickrama, P. W., & Senadheera, S. (2018). Strength and shrink/swell behavior of highly plastic clay treated with geopolymer. *Transportation Research Record, 2672*(52), 174–184.

[18] Fernández-Jiménez, A., & Palomo, Á. (2005). Composition and microstructure of alkali-activated fly ash binder: Effect of the activator. *Cement and Concrete Research, 35*(10), 1984–1992.

[19] Debanath, O. C., Rahman, M. A., Farook, S. M., & Islam, M. R. (2024). Application of ecofriendly geopolymer binder to enhance the strength and swelling properties of expansive soils. *Advances in Civil Engineering, 2024*, 9910728.

[20] Zhang, M., Guo, H., El-Korchi, T., Zhang, G., & Tao, M. (2013). Experimental feasibility study of geopolymer as the next-generation soil stabilizer. *Construction and Building Materials, 47*, 1468–1478.

[21] Cristelo, N., Glendinning, S., Miranda, T., Oliveira, D., & Silva, R. (2012). Influence of curing conditions on the performance of alkaline activated fly ash–soil mixtures. *Journal of Materials in Civil Engineering, 24*(2), 135–144.

[22] Kalina, R. D., Al-Shmaisani, S., Ferron, R. D., & Juenger, M. C. (2019). False positives in ASTM C618 specifications for natural pozzolans. *ACI Materials Journal, 116*(2), 165–172.

[23] Zailani, W., Abdullah, M., Arshad, M., Burduhos-Nergis, D., & Tahir, M. (2020). Effect of iron oxide (Fe_2O_3) on the properties of fly ash-based geopolymer. In *IOP Conference Series: Materials Science and Engineering* (Vol. 743, 012017). IOP Publishing.

[24] Davidovits, J. (2008). *Geopolymer chemistry and applications*. Geopolymer Institute.

[25] Amer, A. A., & El-Hoseny, S. (2017). Properties and performance of metakaolin pozzolanic cement pastes. *Journal of Thermal Analysis and Calorimetry, 129*, 33–44.

[26] Horpibulsuk, S., Rachan, R., Chinkulkijniwat, A., Raksachon, Y., & Suddeepong, A. (2010). Analysis of strength development in cement-stabilized silty clay.

[27] Xu, H., & Van Deventer, J. S. J. (2000). The geopolymerisation of alumino-silicate minerals. *International Journal of Mineral Processing, 59*(3), 247–266.

[28] Duxson, P., Fernández-Jiménez, A., Provis, J. L., Lukey, G. C., Palomo, A., & Van Deventer, J. S. J. (2007). Geopolymer technology: The current state of the art. *Journal of Materials Science, 42*, 2917–2933.

[29] Cristelo, N., Glendinning, S., Miranda, T., Oliveira, D., & Silva, R. (2011). Soil stabilization using alkaline activation of fly ash for self-compacting rammed earth construction. *Construction and Building Materials, 25*(1), 267–276.

[30] Phummiphan, I., Horpibulsuk, S., Phoo-ngernkham, T., Arulrajah, A., & Shen, S. L. (2016). Marginal lateritic soil stabilized with high-calcium fly ash-based geopolymer. *Road Materials and Pavement Design, 17*(4), 877–891.

[31] Provis, J. L. (2009). Activating solution chemistry for geopolymers. In *Geopolymers* (pp. 50–71). Woodhead Publishing.

[32] Abdullah, M. S., & Ahmad, F. (2017). Effect of alkaline activator to fly ash ratio for geopolymer stabilized soil. In *MATEC Web of Conferences* (Vol. 103, 01012). EDP Sciences. https://doi.org/10.1051/matecconf/201710301012

[33] Parhi, P. S., Garanayak, L., Mahamaya, M., & Das, S. K. (2017). Stabilization of an expansive soil using alkali-activated fly ash-based geopolymer. In *Sustainable civil infrastructures: Innovative infrastructure geotechnology* (pp. 36–50). Springer.

[34] Dheyab, W., Ismael, Z. T., Hussein, M. A., & Huat, B. B. K. (2019). Soil stabilization with geopolymers for low-cost and environmentally friendly construction. *GEOMATE Journal, 17*, 271–280.

[35] Shihab, A. M., Abbas, J. M., & Ibrahim, A. M. (2018). Effects of temperature in different initial duration time for soft clay stabilized by fly ash-based geopolymer. *Civil Engineering Journal, 4*, 2082–2096.

[36] Abdila, S. R., Abdullah, M. M. A. B., Ahmad, R., Rahim, S. Z. A., Rychta, M., Wnuk, I., Nabiałek, M., Muskalski, K., Tahir, M. F. M., & Syafwandi. (2021). Evaluation on the mechanical properties of ground granulated blast slag (GGBS) and fly ash stabilized soil via geopolymer process. *Materials, 14*, 2833. https://doi.org/10.3390/ma14112833

[37] Abdila, S. R., Abdullah, M. M. A. B., Ahmad, R., Burduhos Nergis, D. D., Rahim, S. Z. A., Omar, M. F., Sandu, A. V., Vizureanu, P., & Syafwandi. (2022). Potential of soil stabilization using ground granulated blast furnace slag (GGBFS) and fly ash via geopolymerization method: A review. *Materials, 15*, 375.

[38] Sharma, K., & Kumar, A. (2020). Utilization of industrial waste-based geopolymers as a soil stabilizer: A review. *Innovative Infrastructure Solutions, 5*, 97.

[39] Chindaprasirt, P., Jaturapitakkul, C., Chalee, W., & Rattanasak, U. (2009). Comparative study on the characteristics of fly ash and bottom ash geopolymers. *Waste Management, 29*(2), 539–543.

[40] Kumar, B. S. M., Sreenivasulu, C., & Singh, S. P. (2021). Effects of delay time on compaction and strength properties of stabilized granular soil. In *Proceedings of the Indian Geotechnical Conference 2019* (pp. 739–752). Springer.

[41] Mishra, M., Sahoo, P. K., & Singh, S. P. (2021). Plasticity and swelling characteristics of geopolymer-treated expansive soil. In *Proceedings of the Indian Geotechnical Conference 2019* (pp. 195–209). Springer.

[42] *Construction and Building Materials, 24*(10), 2011–2021.

توصيف واستقرار الحجم للطين عالي اللدونة المُثبَّت بواسطة البوليمرات الجيولوجية القائمة على الرماد والميتاكاولين

المستخلص

تهدف هذه الدراسة إلى توصيف وتحليل الخصائص الفيزيائية والكيميائية لتربة طينية من نوع CH، مُثبّتة بشكل مستقل ومنفصل بمخاليط من الجيوبوليمرات المُكوّنة من الرماد المتطاير والميتاكاولين، بنسبة تصل إلى ١٨٪ مُنشّطة بهيدروكسيد الصوديوم. تمّت دراسة أربع نسب مئوية مختلفة من كلا الجيوبوليمرين لتقييم تأثيرهما على لدونة التربة، وتماسكها، وثباتها الحجمي في ظلّ التغيرات الدورية في الرطوبة. تمّ تحليل التركيب الكيميائي لتربة CH والميتاكاولين والرماد المتطاير باستخدام تحليل التألق بالأشعة السينية (XRF) لتقييم كميات الألومينوسيليكات اللازمة لتكوين الجيوبوليمر، ولتأكيد النتائج. أظهرت نتائج حدود أتربيرغ واختبارات التماسك انخفاضًا في لدونة التربة وزيادة في أقصى كثافة جافة لها مع زيادة محتوى الجيوبوليمر. تمّ تقييم المتانة من خلال دورات التمدد والانكماش أحادية البعد، حيث أدّت زيادة محتوى المادة الرابطة إلى انخفاض ملحوظ في تغير الحجم، وبالتالي تحسين الثبات البُعدي نتيجة لتغيرات الرطوبة. أظهر تحليل المجهر الإلكتروني الماسح بنية كثيفة ومتماسكة مع تكوين مستمر لهلام الجيوبوليمر، وتعزيز الترابط بين الجزيئات. تُظهر نتائج هذه الاختبارات أن المواد الرابطة الجيوبوليمرية المنشطة بهيدروكسيد الصوديوم يمكن أن تغير الخصائص الفيزيائية والكيميائية ومصفوفة التربة الطينية لتحسين استقرار أبعادها ومتانة دورة الترطيب والتجفيف.

الكلمات المفتاحية:

التربة الطينية عالية اللدونه؛ الجيوبوليمر؛ الرماد المتطاير؛ الميتاكاولين؛ المنشط القلوي؛ تحسين التربة؛ البنية المجهرية.

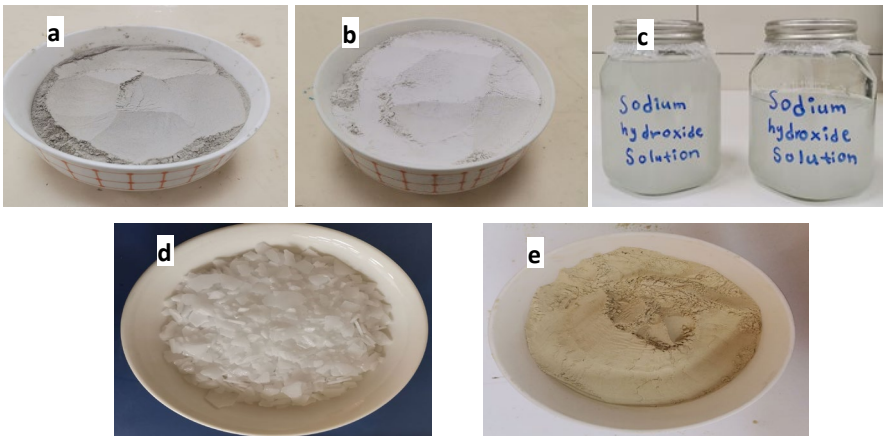

Figure 1: a: fly ash powder, b: metakaolin powder, c: sodium hydroxide solution, d: NaOH flakes, e: bentonite powder.

Product introduction

Product name	HS CODE	CAS.NO	Usage
Calcined Kaolin	2507001000	1332-58-7	Paper and Rubber

Physical properties

Whiteness	Particle Size	Moisture	PH Value
93-94%	2000&4000mesh	≤0.5	6.0-8.0

Figure 2: Production introduction and physical property metakaolin.

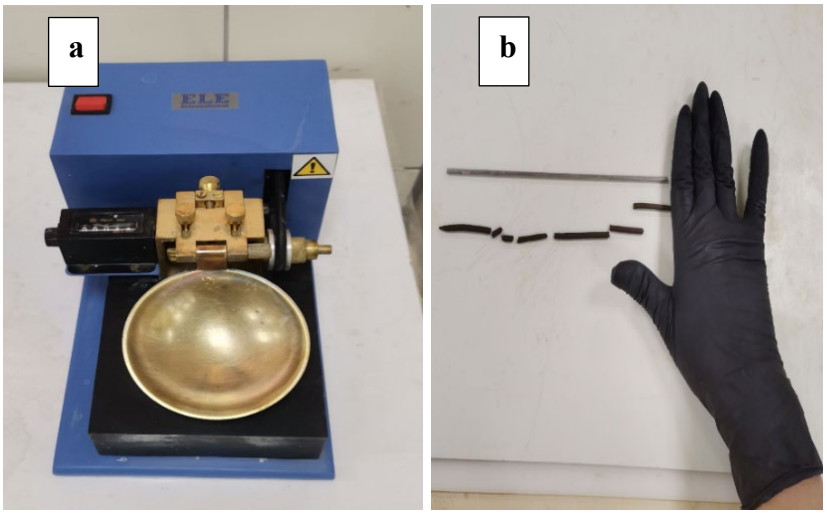

Figure 3: Atterberg limit tests, a: Liquid limit device; b: Plastic limit evaluation.

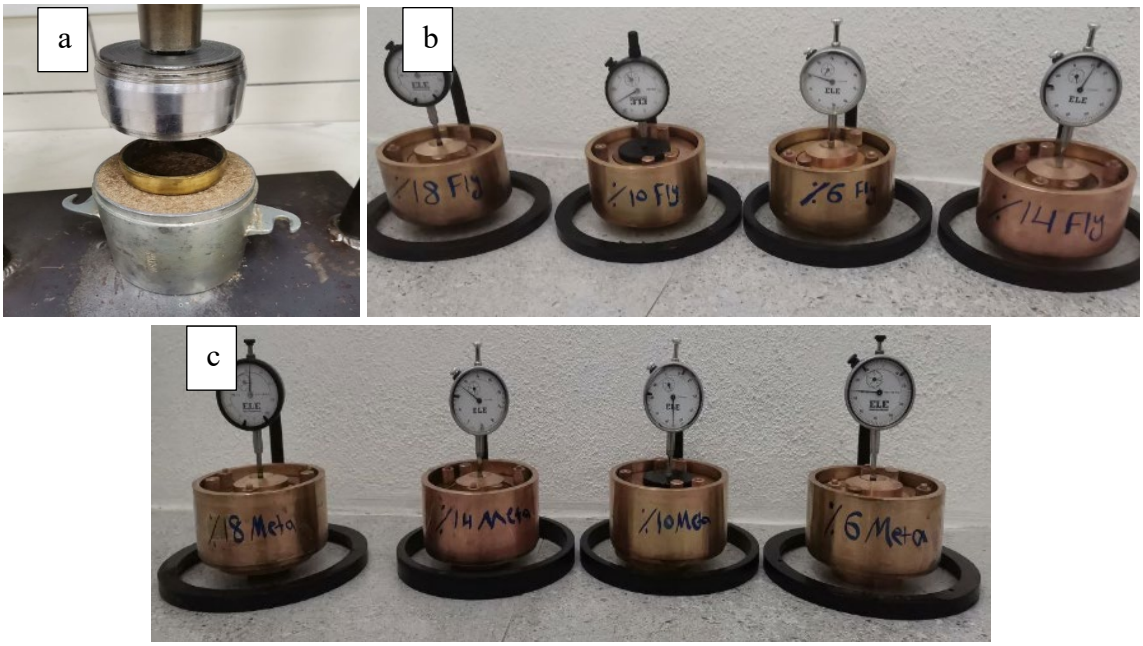

Figure 4: Swell-shrink potential of CH soil: **a:** pressing consolidation ring through compacted soil in compaction mold, **b:** samples for1-D swell-shrink cycles test of fly ash-geopolymer-treated CH soil, and **c:** samples for 1-D swell-shrink cycles test of metakaolin-geopolymer-treated CH soil.

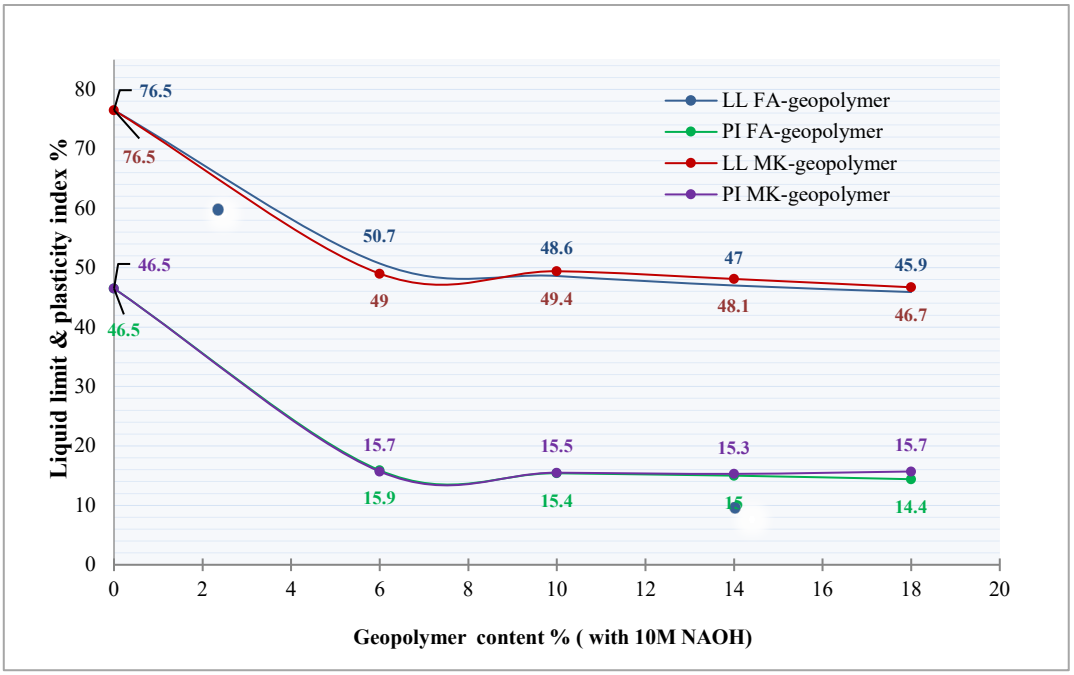

Figure 5 : Effect of fly ash- and metakaolin geopolymers content on the liquid limit and plasticity index of CH soil.

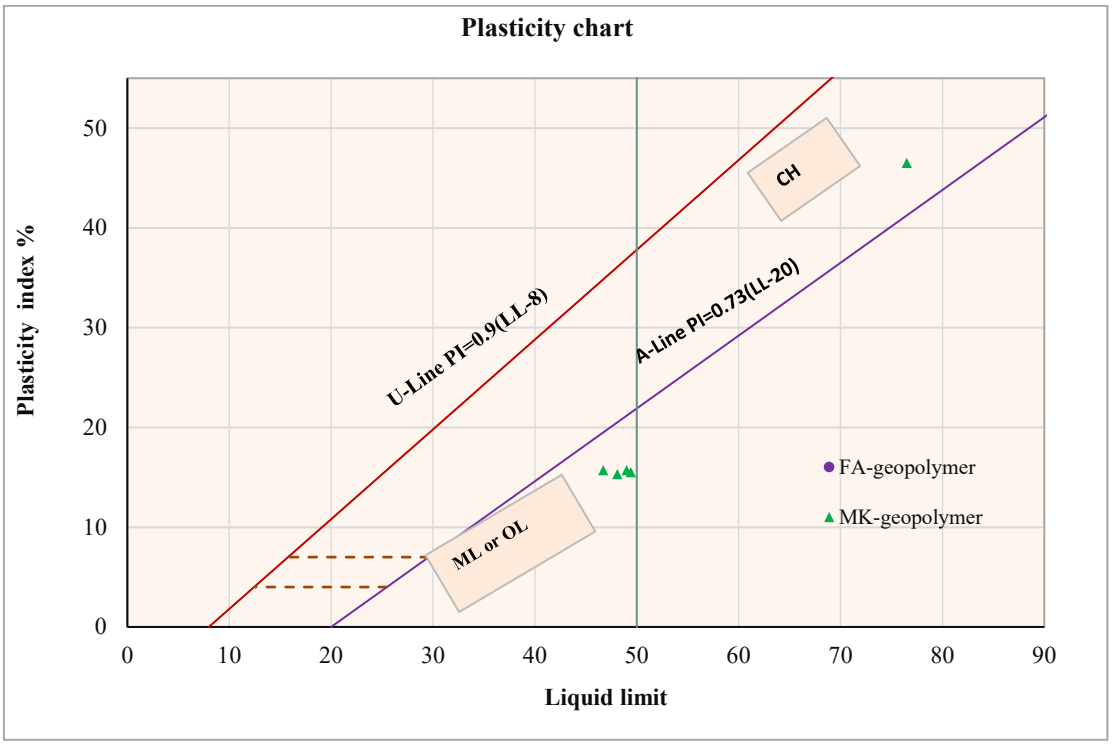

Figure 6: Untreated and treated soil classification in accordance to USCS.

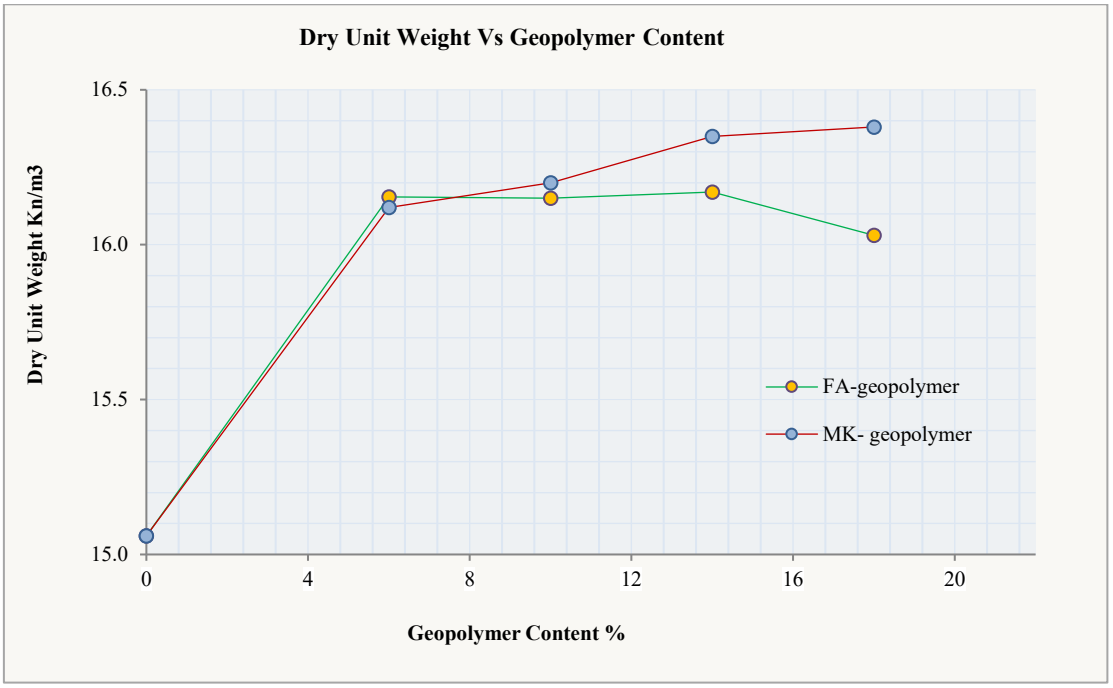

Figure 7: The maximum dry density **(MDD)** vs. geopolymer content for all ratios of metakaolin and fly ash.

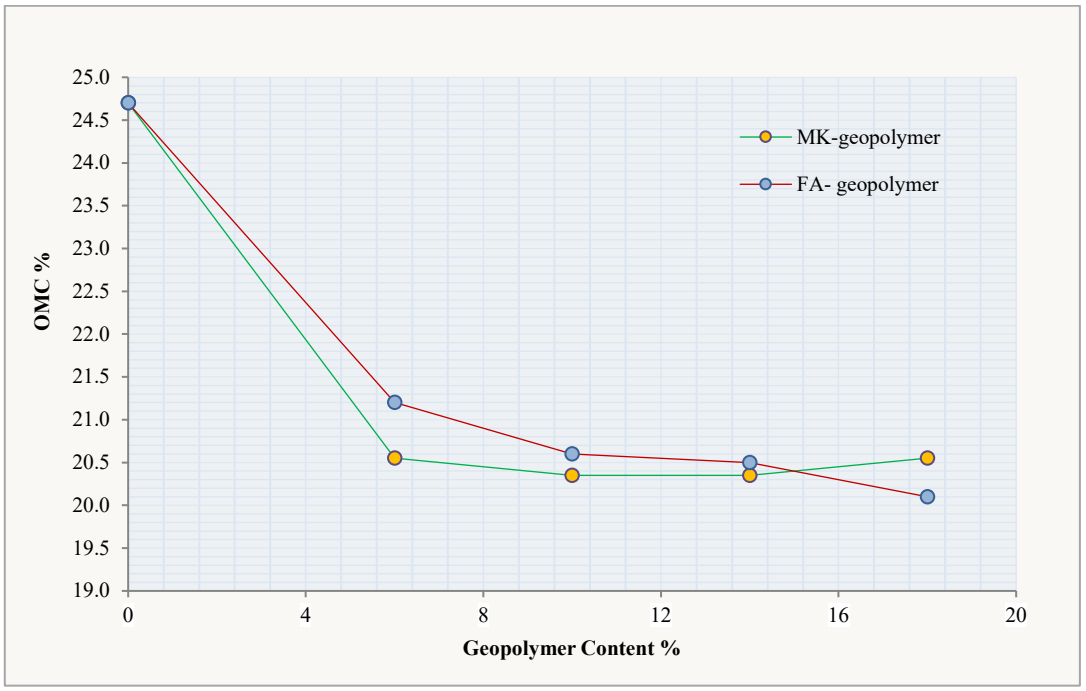

Figure 8: Optimum moisture content (OMC) vs. geopolymer content for all ratios of metakaolin and fly ash.

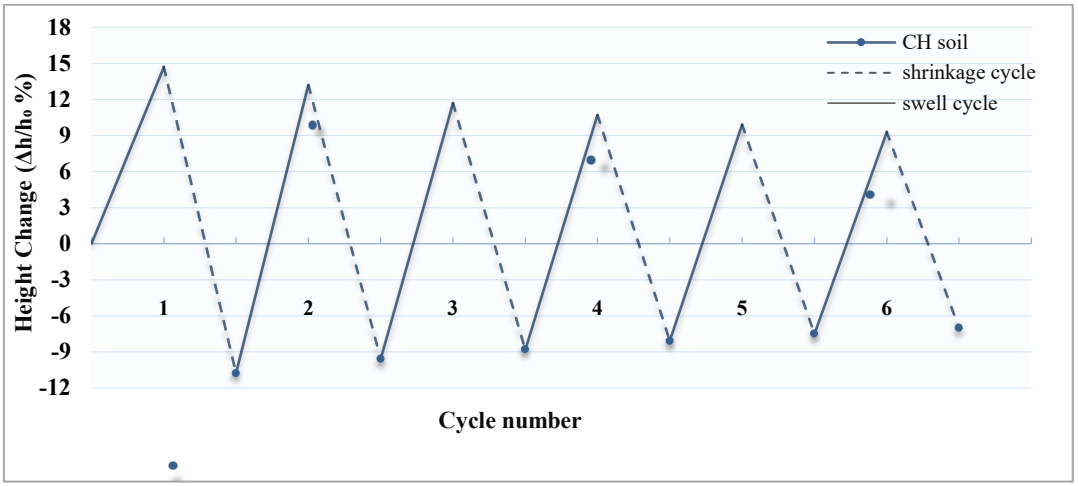

Figure 9: Height Change of CH Soil over 6 Swell-Shrink Cycles.

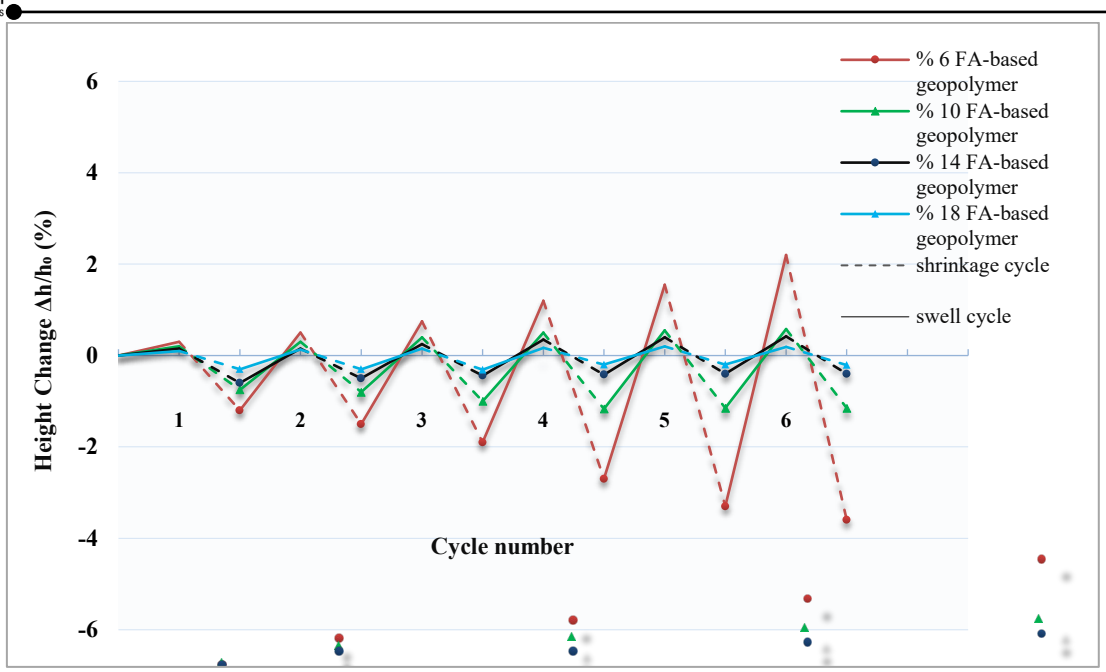

Figure 10: Height Change of Fly Ash–Based Geopolymer over 6 Swell-Shrink Cycles.

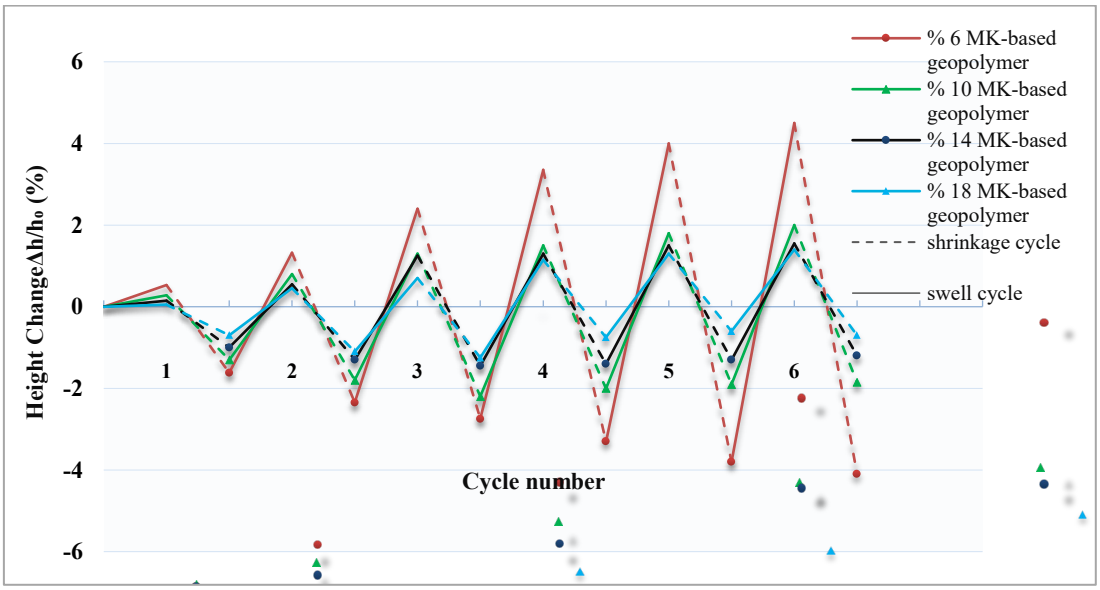

Figure 11: Height Change of Metakaolin-Based Geopolymer over 6 Swell-Shrink Cycles.

Figure 12a: CH soil after 6 swell-shrink cycles.

Figure 12b: 6% FA-geopolymer after 6 swell-shrink cycles.

Figure 12c: 6% MK-geopolymer after 6 swell-shrink cycles.

Figure 12d: 18% FA-geopolymer after 6 swell-shrink cycles.

Figure 12e: 18% MK-geopolymer after 6 swell-shrink cycles.

Figure 12: Performance of Fly Ash and Metakaolin Geopolymer treated HC soil after 6 swell-shrink cycles.

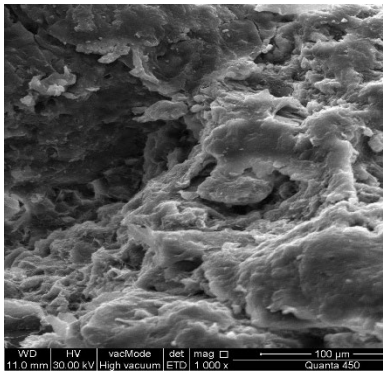

Figure 13a: SEM image of CH soil.

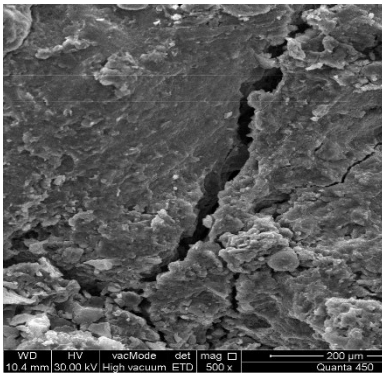

Figure 13b: SEM image of CH soil after 6-swell-shrink cycles.

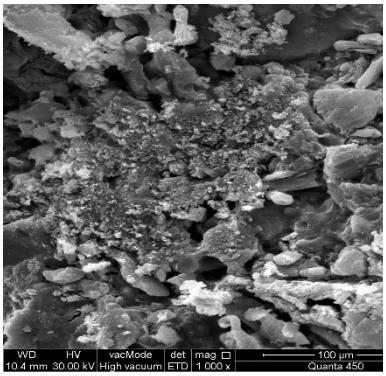

Figure 13c: SEM images of CH soil after 6-swell-shrink cycles.

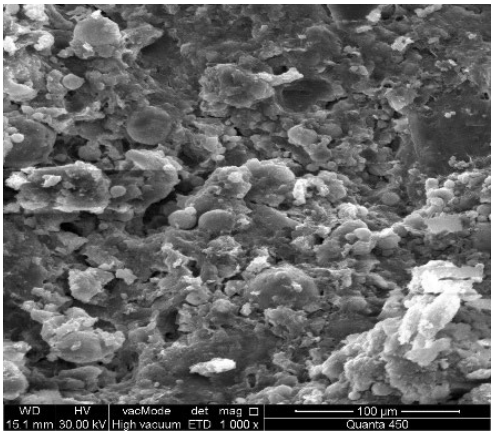

Figure 13d: SEM images of 18% fly ash-geopolymer–stabilized CH soil.

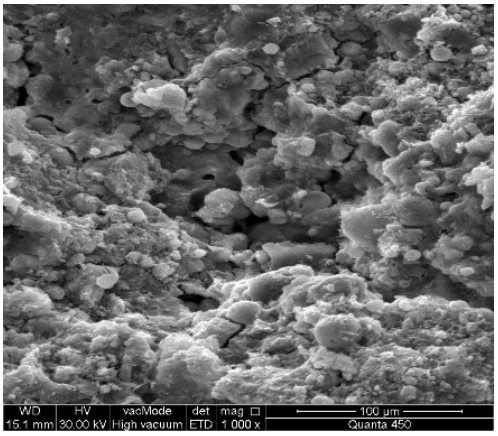

Figure 13e: SEM image of 18% fly ash–geopolymer–stabilized CH soil after 6-swell-shrink cycles.

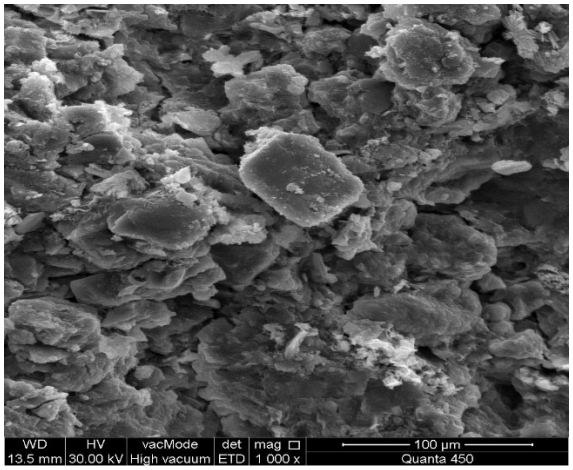

Figure 13f: SEM image of 18% metakaolin–geopolymer–stabilized CH soil.

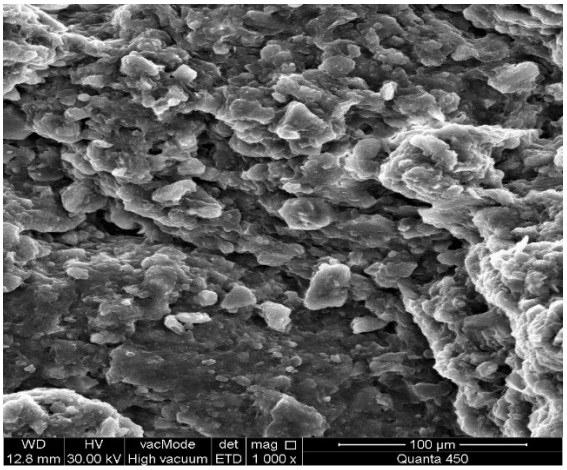

Figure 13g: SEM image of 18% metakaolin–geopolymer–stabilized CH soil after 6-swell-shrink cycles.

Figure 13: SEM image of different swell-shrink cycles.

Table 1: Soil Properties

Property	Test Method (ASTM)	value
Gravel (%)	ASTM D422	0.2
Sand (%)	ASTM D422	11.4
Silt (%)	ASTM D422	36.4
Clay (%)	ASTM D422	52.0
Percent passing No.200	ASTM D422	88.4
Specific gravity (Gs)	ASTM D854	2.52
Liquid limit (%)	ASTM D4318	76.5
Plastic limit (%)	ASTM D4318	30
Plasticity index (%)	ASTM D4318	46.5
Unified Soil Classification System (USCS)	ASTM D2487	Fine grained; CH
Optimum moisture content (%)	ASTM D698	24.7
Maximum dry density (kN/m³)	ASTM D698	15.06
Unconfined compressive strength (kPa)	ASTM D2166	467
Free Swell percentage (%)	ASTM D4546	14.7
Swell pressure (kPa)	ASTM D4546	275

Table 2: Chemical Compostion (Fly Ash, Metakaolin, CH Soil, 6% - 18%Fly Ash+CH Soil, 6%-18% Metakaolin+CH Soil).

Name	MgO (%)	Al_2O_3 (%)	Fe_2O_3 (%)	SiO_2 (%)	K_2O (%)	CaO (%)	OTHERS (%)
CH Soil	6.757	18.1720	7.8799	59.0499	2.2167	5.5062	0.4182
Fly Ash	1.9742	26.6766	3.8339	64.0602	1.1874	1.5727	0.695
Metakaolin	5.2398	19.6744	0.9949	70.5502	2.0301	1.0285	0.4821